Desalination and Water Treatment
www.deswater.com

doi: 10.5004/dwt.2021.27594

233 (2021) 158–169
September

Sodium acetate functionalized timber sawdust for effective removal of cadmium ions and basic/acid dyes from aqueous solutions

Meriem Bendjelloul[a,b,*], El Hadj Elandaloussi[b,*], Louis-Charles de Ménorval[c]

[a]*Laboratoire de Valorisation des Matériaux, Université Abdelhamid Ibn Badis, B.P. 227, 27000 Mostaganem, Algeria, email: meriem.bendjelloul@univ-relizane.dz (M. Bendjelloul)*
[b]*Department of Chemistry, Faculty of Sciences & Technology, Ahmed Zabana University–Relizane, Bourmadia, 48000 Relizane, Algeria, email: elhadj.elandaloussi@univ-relizane.dz (E.H. Elandaloussi)*
[c]*ICG–AIME–UMR 5253, Université Montpellier 2, Place Eugène Bataillon CC 1502, 34095 Montpellier Cedex 05, France*

Received 22 March 2021; Accepted 5 July 2021

ABSTRACT

This work was set to add value to timber sawdust through its functionalization with acetate groups for the sorption of cadmium ions and basic/acid dyes in aqueous solutions, as a cost-effective process. Straightforward etherification of the lignocellulosic matrix of sawdust with sodium chloroacetate yielded SATS material, which was characterized and successfully used as an excellent adsorbent for efficient removal of cadmium ions, Bezaktiv Marine S-BL, Indigo Carmine from aqueous solutions. The as-prepared SATS demonstrated remarkable adsorption performance for all pollutants at pH 6 and the adsorption capacities of Cd^{2+}, BM and IC were approximately 204, 200 and 142.8 mg g^{-1}. Thermodynamic parameters indicated the exothermic and spontaneous nature of the removal process. Satisfactory adsorption behavior including fast adsorption kinetics, high adsorption capacity, competitive ions and excellent properties of rapid adsorption/desorption rates remained during the repeated cycles demonstrated the large potential of SATS sorbent material for effluent treatment applications. Proposed adsorption mechanism indicated that ion-exchange is involved in Cd(II) removal, whereas electrostatic interaction and surface complexation may also contribute to the removal of dyes.

Keywords: Lignocellulosics; Acetate linkers; Cadmium ions; Bezaktiv marine S-BL; Isotherms

1. Introduction

Contamination of water systems with heavy metals and synthetic chemicals is one of the most significant environmental concerns [1,2]. Heavy metal pollution of aquatic ecosystems is mainly due to the discharge of untreated metal-containing effluents into water bodies by industries such as batteries and electroplating [3]. Among heavy metals, cadmium has attracted great attention as its residual toxicity can significantly affect both environment and public health [4,5]. On the other hand, the contamination of water systems by the increasing production and use of synthetic chemicals such as dyes by textile, leather and dyeing industries, poses a significant risk to human health and aquatic organisms [6–8]. Therefore, it is crucial to remove these pollutants from industrial effluents before they are released into the environment.

Several treatment strategies are available for the removal of heavy metals and synthetic dyes in wastewater, which include chemical precipitation [9], membrane separation [10], oxidation [11], Fenton process [12]. Photodegradation is a well-known method for effective and fast removal of dyes from water. However, photo-catalytic degradation process often requires the aid of UV light

* Corresponding authors.

irradiation to enhance the photocatalytic activity and promote the degradation efficiency of dyes [13,14]. Although these processes have advantages, they often require complex equipment and high operational costs. In addition, they lead often to partial removal, and may even generate secondary pollution. In this context, adsorption is considered as a promising alternative for its ease and simplicity in the process design. Owing to their well-developed microporosity and surface chemistry, activated carbons are very effective in removing metal ions and organic pollutants from water [15,16]. However, the removal process by means of activated carbon is costly. From this perspective, the use of industrial by-products and agricultural wastes as adsorbents has drawn great interest as they remove a wide variety of both mineral and organic pollutants and generates less toxic products than many other remediation methods [17–22]. Bio-based adsorbents such as egg shell [23] or biosorbents derived from agricultural wastes such as hazelnut shells [24], olive stones [25] and other cellulosic materials [26] have been thoroughly investigated in the removal of heavy metals and organic pollutants in water.

Lignocellulosic wastes have been successfully used as low-cost bioadsorbents owing to their wide availability, biodegradability, low cost, low toxicity, regenerability, and lower sludge generation. Thanks to the large variety of functional groups available at their surface, lignocellulosic wastes are able to bind with both heavy metal ions and organic pollutants [27,28]. Therefore, chemical modification of lignocellulosic wastes is an attractive approach that allows the synthesis of materials with desired functionalities designed for a significant enhancement of the adsorption capacity.

The purpose of this work was set to valorize a by-product of the timber industry by chemical modification. Taking into account the abundant surface hydroxyl groups on the lignocellulosic matrix of timber sawdust, etherification by means of sodium chloroacetate could be an effective method to introduce plenty of adsorption sites on the resulting etherified material. We hypothesized that the incorporation of linkers bearing negatively charged sodium acetate sites within the lignocellulosic matrix should provide an excellent sorption property, involving ion exchange and/or electrostatic interactions, especially for heavy metals and ionic organic dyes.

Herein, we developed an efficient and simple procedure to prepare a functionalized timber sawdust material (SATS) bearing sodium acetate groups for the removal of targeted pollutants. In view of the complex chemical composition of the timber sawdust, we first proceeded to an alkaline treatment of the material with aqueous sodium hydroxide solution to further enhance the reactivity of hydroxyl groups. This processing also permits the removal of base soluble extractives and part of the lignin from the sawdust [29,30], and eventually facilitates the grafting of carboxylate groups onto the lignocellulosic matrix. Etherification of the alkali-treated timber sawdust (ATTS) with sodium chloroacetate was performed to yield the functionalized timber sawdust bearing sodium acetate linkers (SATS). The as-prepared adsorbent material was characterized and then evaluated for its capacity to remove basic and acid dyes, Bezaktiv marine S-BL (BM) and indigo carmine (IC), respectively, and cadmium ions from water. The three pollutants were selected because of their wide use and presence in industrial wastewaters. Besides, there are no published studies on the removal of bezaktiv marine S-BL dye, which limits the comparison of our results with other work. A series of sorption experiments under different conditions, that is, effect of initial pH, kinetics, isotherms, ionic strength, and effect of temperature were conducted to investigate the adsorption behavior and performance of the three pollutants. In addition, the role of functional acetate groups linked to the surface of SATS, in the sorption of Cd(II) and the dyes, was examined by esterification of acetate groups to identify a sorption mechanism. Finally, the regeneration and reusability of SATS has been carefully examined to ascertain its stability.

2. Materials and methods

2.1. Chemicals

Timber sawdust (TS) as received from a local carpenter was thoroughly washed with hot distilled water, then with acetone. The material was dried in an oven at 100°C until constant weight, and was sieved for a particle size of 250 μm. Basic bifunctional dye Bezaktiv Marine S-BL was kindly provided by a textile company, Indigo carmine (IC) anionic dye and cadmium nitrate $Cd(NO_3)_2{\cdot}4H_2O$ were purchased from Prochima-Sigma, (Tlemcen, Algeria). All chemicals were of analytical grade and used as received without further purification. Stock solutions (1,000 mg L^{-1}) of each pollutant were prepared by dissolving Bezaktiv marine S-BL, indigo carmine and $Cd(NO_3)_2{\cdot}4H_2O$ in distilled water. Test solutions of desired concentrations were obtained by further dilution with distilled water. Dyes and Cd(II) solutions of desired pH values were obtained by adjustment using either dilute HCl (0.1 N) or NaOH (0.1 N) solutions.

2.2. Synthesis of SATS

SATS adsorbent containing sodium acetate groups was prepared by reaction of the ATTS with sodium chloroacetate in toluene-pyridine mixture. First, the alkaline treatment of timber sawdust was conducted by immersing at once 50 g of TS in 500 mL of 20 wt.% sodium hydroxide solution. The resulting mixture was stirred overnight at room temperature. The suspension was filtered and the solid was thoroughly washed with distilled water until neutral pH was obtained. The solid was then re-suspended in 300 mL of 1 M HCl aqueous solution and left to magnetic stirrer for 24 h. After filtration, the solid was washed several times with distilled water and then with acetone and finally dried in an electric drying oven at 80°C. The material was passed through a 250 μm sieve to afford 23 g of ATTS as a yellowish powder. To a suspension of ATTS (10 g) and pyridine (30 mL) in toluene (200 mL) heated at 60°C was added at once sodium chloroacetate (15.3 g). The resulting mixture was left to stir overnight at 80°C. After cooling, the solid was filtered off, washed thoroughly with water to remove the unreacted sodium chloroacetate and then with acetone. The solid was dried to yield SATS (12.35 g) as a dark-brown solid, which was sieved to a particle size of 250 μm.

2.3. Blocking of acetate groups on the surface of SATS by esterification

To a suspension of 1 g of SATS in 25 mL of dry acetone was added excess of iodomethane (10 mL) and the mixture was stirred for 4 h at 35°C. Excess CH_3I and the solvent were evaporated and the residue was thoroughly washed with distilled water to remove sodium iodide by-product and then with acetone. The methyl acetate ester material (MATS) was dried and sieved to a particle size of 250 μm.

2.4. Sorbent characterization

The pH corresponding to the point of zero charge for SATS and the methyl ester (MATS) was determined by the pH drift method [31]. The structure of SATS material was determined by several characterization methods. The Fourier transform infrared (FTIR) spectra were collected using a Nicolet Avatar 330. ^{13}C cross polarization magic angle spinning nuclear magnetic resonance (CP/MAS NMR) spectra were recorded on a Bruker 300 (Digital NMR Avance) spectrometer (Bruker, USA). UV-Visible absorption spectra of powder samples were recorded on a U-2900 Spectrophotometer. The powder X-ray diffractograms (Philips X'Pert MPD diffractometer , Netherlands) of the samples were analyzed using CuKα radiation (λ = 1.5418 Å) at a scan rate of 0.2°/min with a 2θ scan range of 3.5°–70°. SEM images of the samples were collected using a HITACHI S-4800 SEM (Japan). The thermal stability of the samples were analyzed via thermogravimetric analyses (TGA) using a NETZSCH STA 409 PC/PG simultaneous thermal analyzer (Germany) at a heating rate of 10°C/min under nitrogen atmosphere.

2.5. Adsorption experiments

A series of adsorption experiments were conducted by preparing solutions of Cd(II) and dyes compounds in distilled water at different initial concentrations ranging from 20 to 800 mg/L. Equilibrium studies for a single metal or dye systems were conducted by agitating 25 mg of adsorbent (SATS) with 25 mL of pollutant solution of desired concentration in 100 mL stoppered conical flask up to equilibrium time. SATS sorbent concentrations were 1 g/L for all pollutants. All studies were conducted at room temperature on a stirring plate adjusted to a 100 rpm stirring rate for 60 min. To observe pH effect, the adsorption experiments were carried out at the pH range of 2–10, adjusted by adding aliquots of 0.1 M NaOH and/or HCl prior to adding SATS into the solution. The highest adsorption performance was observed at pH 6 for cadmium as well as for indigo carmine and bezaktiv marine. Thus, the solution pH of 6 was chosen for all other adsorption experiments. After equilibrium, solutions were collected and separated through a 0.2 μm syringe filter, and the aqueous concentrations of dyes compounds were analyzed using a JASCO V-730 UV–visible spectrophotometer (France) at a specific wavelength of 601 and 610 nm for BM and IC, respectively. The residual concentrations of Cd(II) were analyzed by flame atomic absorption spectrophotometer (Pye Unicam SP9 model, UK) equipped with air–acetylene flame at 228.8 nm. The sorbed concentrations of metal ions and dyes at equilibrium were calculated using the following equation:

$$q_e = \frac{\left(C_i - C_e\right) \times V}{w} \tag{1}$$

where q_e is the amount (mg g^{-1}) of pollutant sorbed, C_i and C_e are the initial and equilibrium pollutant concentrations (mg L^{-1}) in solution, respectively, V is the adsorbate volume (L) and w is the sorbent weight (g).

The kinetic experiments were also performed at pH 6 with similar equipment and conditions. The sorbent mass was 25 mg, and the volume of the pollutant solution was 25 mL (20 mg L^{-1}) in this series of tests. Over the experiment, the solution samples were collected at different time intervals of 2–60 min. At predetermined times (i.e., at 2, 4, 6, 8, 10, 15, 20, 25, 30, 40, 50 and 60 min), the samples were withdrawn and were analyzed for the residual pollutant concentration. The influence of temperature on the removal process was studied at three different temperatures (25°C, 35°C and 45°C) with SATS suspensions in Cd(II), BM and IC solutions (20 mg L^{-1}). The suspensions were stirred during 60 min, and then the pollutants concentrations were analyzed. The influence of ionic strength on the sorption process was monitored with SATS suspensions in BM and IC solutions (20 mg L^{-1}) by varying the concentration of sodium chloride from 0 to 5 mol L^{-1}. The mixtures were stirred for 60 min and then were drawn for dye concentration analysis. All measurements were performed in duplicate, yielding an experimental error of less than 2%.

2.6. Desorption and reusability of SATS

400 mg of SATS was dispersed into 400 mL of Cd(II), BM and IC (20 mg L^{-1}, pH 6). After 60 min of contact time, the exhausted SATS materials were washed with distilled water, air dried, and then suspended either in 400 mL of aqueous 1 M NaCl solution for Cd^{2+}, or 1 M NaOH for BM or in 50 mL of $EtOH/H^+$ solution for IC. The mixtures were thoroughly stirred during 60 min for Cd(II) and 15 min for BM and IC-loaded SATS. Afterward they were centrifuged for adsorbate determination in the supernatant. The collected adsorbent was used in the next adsorption–desorption cycle after being thoroughly washed with distilled water and air dried.

3. Results and discussion

3.1. Characterization of SATS adsorbent

FTIR spectra of the precursor ATTS and the functionalized SATS material are shown in Fig. 1. Compared with the precursor ATTS sample, SATS spectrum showed a distinctive intense absorption band at 1,752 cm^{-1} corresponding to the stretching vibration of C=O bonds of carboxylate groups. This gives a clear evidence for the occurrence of etherification reaction of hydroxyl groups of timber sawdust with sodium chloroacetate. The large absorption band at 3,399 cm^{-1} can be assigned to the stretching band of both carboxylate and alcohol groups. The band at 2,910 cm^{-1} is characteristic of C–H stretching of the methylene group of the lignocellulosic material [32]. The absorption band at 1,623 cm^{-1} may be attributed to the

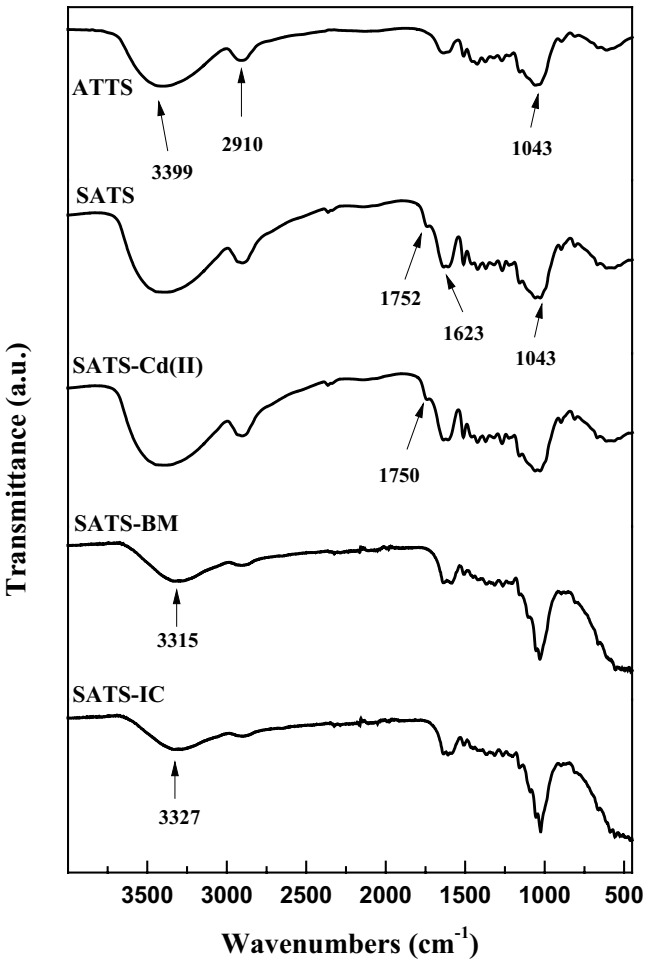

Fig. 1. Fourier transform infrared spectra of the alkali-treated timber sawdust and the synthesized SATS before and after Cd(II), BM and IC adsorption.

C=C stretching of the aromatic rings of the lignin fraction. The strong absorption band observed at 1,043 cm^{-1} is characteristic of C–O–C bond stretching of ether groups.

FTIR spectrum of Cd(II)-sorbed SATS showed that the peak expected at 1,752 cm^{-1} had slightly shifted to 1,750 cm^{-1}, due to Cd^{2+} sorption (Fig. 1). This shift may be attributed to the exchange of counter ions associated with acetate anions, suggesting that negatively charged carboxyl groups are predominant contributors in metal ion uptake. On the other hand, dyes-SATS FTIR spectra were clearly different from the SATS FTIR spectrum. The characteristic carbonyl group absorbance peak at 1,752 cm^{-1} disappeared in dyes-SATS spectra due to strong binding affinities of dyes for carboxyl groups. The carbonyl stretching peak has probably shifted to a lower wavelength after the sorption of dyes, indicating the reduction of electron density around the oxygen atom due to the formation of H bonds with organic dyes molecules. In addition, the peak at 3,399 cm^{-1} identified as the stretching vibration of O–H was shifted to 3,315 and 3,327 cm^{-1} after adsorption of BM and IC, respectively. Moreover, the absorption band weakened completely, which indicates the interaction of –OH with BM and IC dyes. These results indicated synergistic effects between electrostatic attraction and hydrogen bonding between the surface of SATS material and dyes molecules.

Moreover, as shown in Fig. 2a, MAS ^{13}C NMR spectra of ATTS and SATS materials also confirm the grafting of acetate groups onto the lignocellulosic matrix of timber sawdust.

The spectrum of the lignocellulosic ATTS material shows signals from 61.6 to 104.5 ppm attributable to the six carbon atoms of the glucose unit of cellulose. The spectrum also revealed weak signals appearing at 135–145 ppm, which can be assigned to aromatic rings of the residual lignin subsequent to the alkaline treatment of sawdust. On the other hand, after etherification, the spectrum of SATS displays two extra peaks characteristic of acetate functional groups at 174 and 64.5 ppm, which correspond to the carbonyl carbon atoms C=O (carboxylic acid) and CH_2 (methylene), respectively. In addition, the basic character of SATS revealed by the pH_{PZC} value (8.5) along with the total number of acetate groups (3.73 mEq g^{-1}) determined by titration, provide unequivocal evidence that the etherification reaction has indeed taken place.

The UV-Vis absorption spectra of SATS before and after adsorption of BM and IC dyes are shown in Fig. 2b. All the spectra revealed well resolved characteristic absorption peaks of the functional lignocellulosic material for all the samples. The main absorption peak located at 232 nm for SATS can be assigned to UV chromophore functional groups of the cellulosic material whereas the peak at 412 nm is undoubtedly attributed to unsaturated functional groups of lignin including conjugated carbonyl groups, aromatic rings and carbon–carbon double bonds. However, in dyes-SATS samples, the absorption peak at 232 nm is blue-shifted to 211 nm on BM and IC sorption. In addition, as the sorption of dye occurs onto SATS, the absorption peak shifted towards higher wavelengths (up to 629 nm). The peaks in the absorption spectra do not correspond to the true wavelengths of the dyes, which are about 601 and 610 nm for BM and IC, respectively. To sum up, these results revealed that the acetate linkers are the main functional groups in SATS material that are likely to participate in dyes binding.

The powder X-ray diffraction patterns of ATTS and SATS are shown in Fig. 3. Prior to etherification with sodium chloroacetate, the X-ray scattering diagram of ATTS showed one main diffraction ray for 2θ value of 20.9°, which is due to presence of crystalline cellulose in the timber sawdust sample [33]. Nevertheless, after functionalization with acetate linkers, the ray of the crystal lattice was shifted to 2θ value of 22.3° and narrowed. A second new ray, weaker in intensity and located at 2θ value of 16° gives an evidence of the grafting of acetate functional groups onto the lignocellulosic matrix.

TGA curves of ATTS and SATS materials are shown in Fig. 4. The initial gradual weight loss of both ATTS and SATS materials decreased by 12% at approximately 100°C indicated the moisture evaporation. After 100°C, the weight remained constant until the initial temperature of combustion was reached. The combustion profiles of the samples indicated a slightly higher thermal stability for SATS than the alkali-treated timber sawdust (ATTS). The initial temperature of ATTS combustion was 201°C. However, the effect of acetate functionalization was

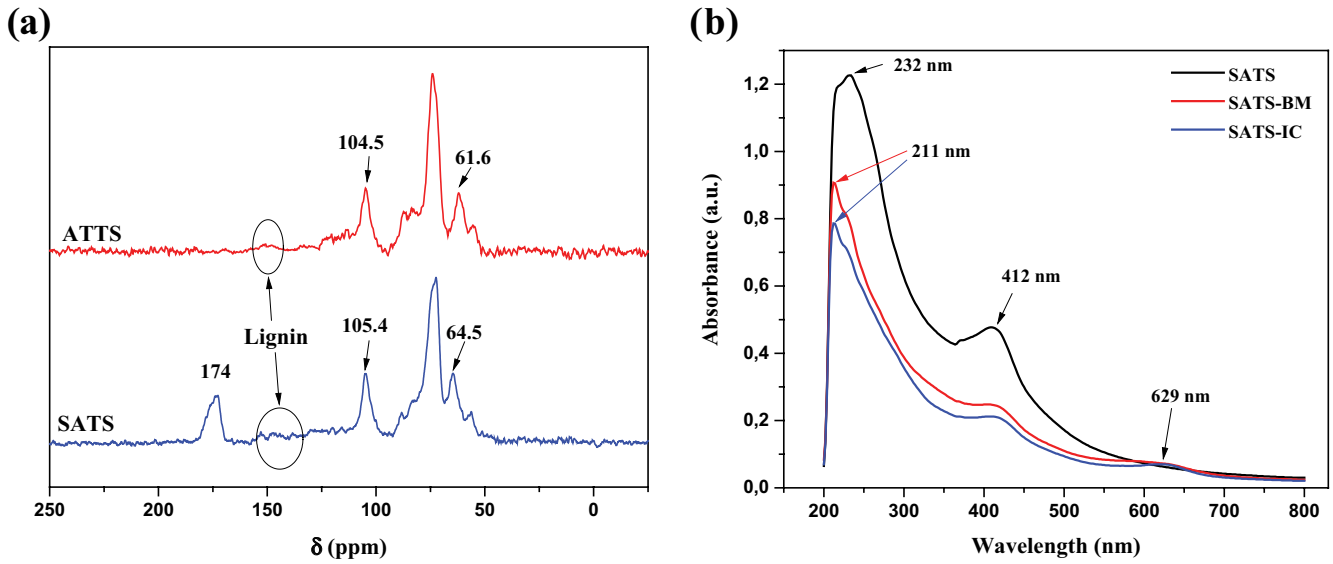

Fig. 2. Solid-state CPMAS ^{13}C NMR spectra of ATTS and SATS (a); solid UV-visible spectra of SATS and BM and IC loaded SATS (b).

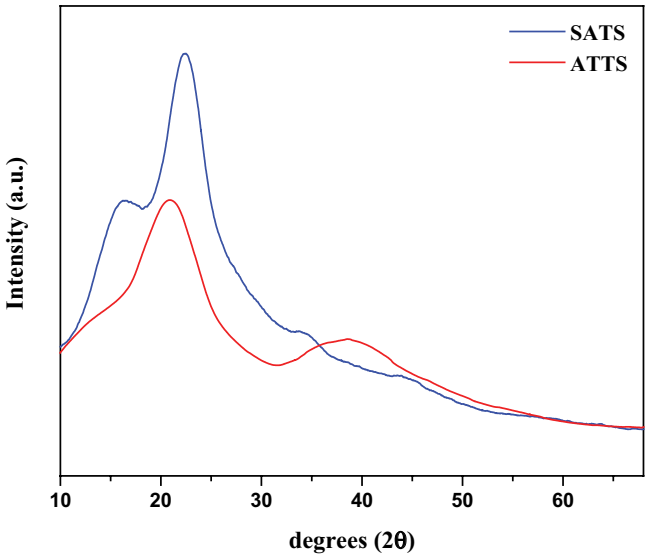

Fig. 3. Powder X-ray diffraction pattern of ATTS and SATS.

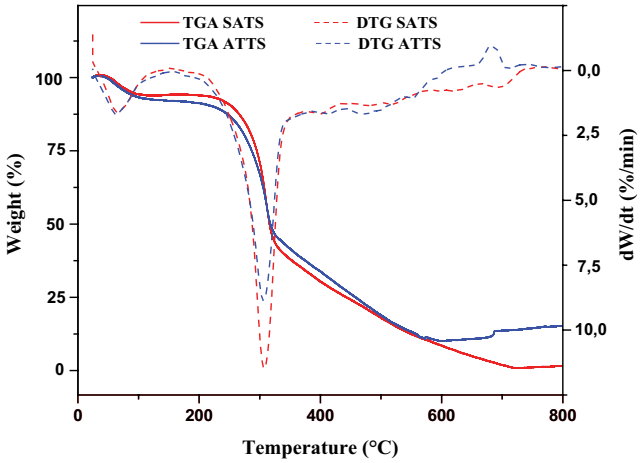

Fig. 4. Thermogravimetric analyses responses of ATTS and SATS at a rate of 10°C/min, in nitrogen and their derivatives.

apparent for SATS whose initial temperature of combustion was at 210°C. During this stage, both ATTS and SATS were almost totally burnt out due to the destruction of the crystalline structure and oxidative thermal degradation. The degradation of hemicelluloses partially overlaps with cellulose degradation in the timber sawdust, and lignin degradation occurs within the temperature range of 200°C–700°C [34]. The maximum weight loss of the samples occurred at 308°C, due to the thermal degradation of cellulose. The weight loss stopped at higher combustion temperature, and some residual carbon materials remained for ATTS and SATS samples.

SEM images of ATTS and SATS samples are shown in Fig. 5. Micrographs of ATTS and SATS samples (Figs. 5a and c) show a broad variety of jagged and irregular particles of different size and shape, which are characteristic of sawdust. Fig. 5b shows a rather smooth surface for the ATTS sample with no apparent pores or cracks. Although the etherification of the alkali-treated sawdust did not produce a significant change in its surface morphology, nevertheless the surface of the SATS sample became slightly uneven after functionalization with acetate linkers (Fig. 5d). The confirmation of Cd^{2+}, BM and IC adsorption onto SATS material was performed by surface morphology study carried out by SEM (Figs. 5e–g). The images show the stuffing of pollutants onto the surface of SATS adsorbent.

3.2. Removal of cadmium ions, bezaktiv marine and indigo carmine using SATS

The sorption capacity of SATS material was investigated using cadmium ions (Cd^{2+}) and bezaktiv marine (BM) as model cationic pollutants that have seemingly high affinity with the basic acetate functional groups linked to the surface of the adsorbent. Moreover, in spite of its basic

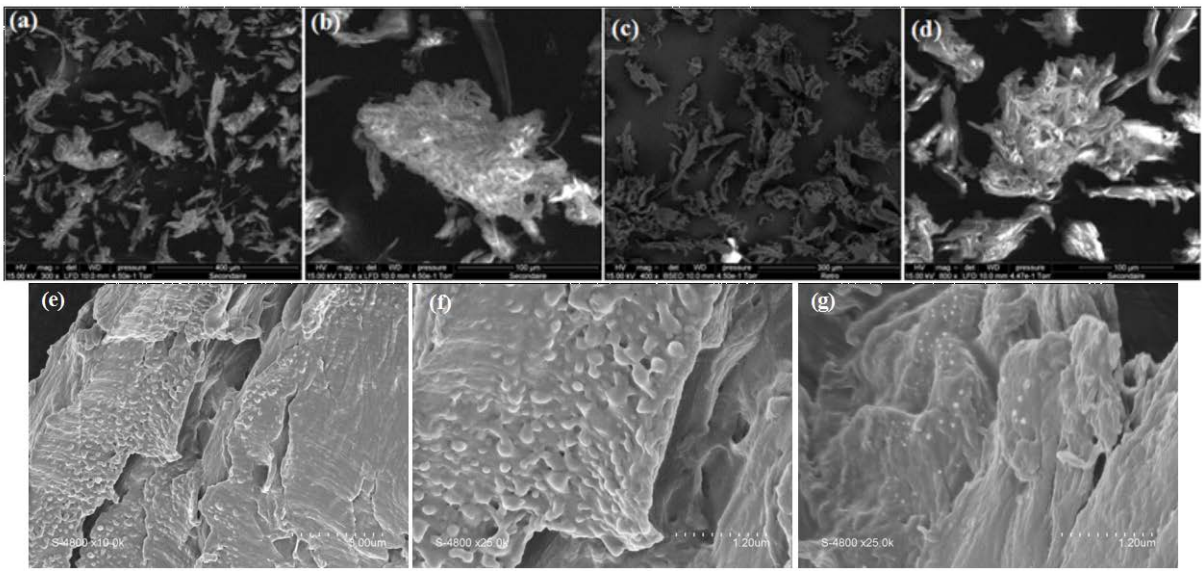

Fig. 5. SEM images of ATTS (a,b), SATS (c,d) and Cd^{2+}, BM and IC loaded SATS (e,f,g).

character, the sorbent material was also evaluated for its capacity to remove an anionic dye, that is, indigo carmine (IC).

First, the influence of the solution pH on adsorption capacity of SATS was investigated within a wide pH range (2–10). As shown in Fig. 6a, the pH has nearly no effect on the adsorption of cadmium ions and bezaktiv marine when the pH increased from 6 to 10. However, a decrease in adsorption performance was observed at pH 2 and pH 2–4 for BM and Cd(II), respectively. This is indubitably inherent to the higher concentrations of competing protons in water with cationic pollutants for sorption onto the basic acetate sites of the adsorbent. Nevertheless, low pH values influence greatly the sorption capacity for cadmium ions than for cationic BM dye. Fig. 6a shows that Cd^{2+} and BM uptake increases strongly with the increase of pH, since at higher pH values, more sodium acetate groups are available for metal binding and competition for the active sites between H^+ and Cd^{2+} or BM dye decreases due to the lower proton concentration. Summing up, the adsorption performance for Cd^{2+}, BM and IC is quite steady over the pH range of 6–10 and the removal rate is substantially high (98%) for cadmium ions and even quantitative for bezaktiv marine (100%). On the other hand, the indigo carmine sorption onto SATS adsorbent sharply decreased as the pH increased from 6 to 10. Beyond pH 6 and taking into account the pH_{PZC} value of SATS (8.5), it was expected that IC dye would be less adsorbed due to the highest electrostatic repulsive interactions between the anionic dye molecules and the negatively charged surface of the adsorbent. However, at a very low pH (2–4), the concentration of H^+ in the bulk solution would be high and the acetate, hydroxyl groups of SATS would be protonated, thus enhancing the electrostatic attraction between adsorbent and IC.

The above results suggest that high adsorption performance was observed at pH 6 for the three investigated pollutants. Thus, all the subsequent adsorption experiments were carried out at pH 6. The Cd(II), BM and IC adsorption isotherms for SATS (Fig. 6b) are characterized by a regular shape with a steep initial slope. The great affinity of the adsorbent for all three pollutants is suggested by the quantitative uptake at low adsorbate concentrations.

The experimental data were fitted to both Langmuir and Freundlich isotherm models. The Langmuir isotherm model suggests the homogeneous monolayer adsorption of adsorbate on independent binding sites of the sorbent surface, and is written as Eqs. (2) and (3):

$$q_e = \frac{q_m b C_e}{1 + b C_e} \qquad \text{(non-linear form)} \tag{2}$$

$$\frac{C_e}{q_e} = \frac{C_e}{q_m} + \frac{1}{q_m b} \qquad \text{(linear form)} \tag{3}$$

where q_e (mg g^{-1}) indicates the sorption capacity at equilibrium, q_m represents the maximum sorption capacity of the adsorbent, C_e is the adsorbate concentration at equilibrium (mg L^{-1}) and b represents the Langmuir affinity constant (L mg^{-1}).

On the other hand, the adsorption data were also fitted to the Freundlich model, which describes the adsorption of adsorbate over a reversible multilayer adsorption on heterogeneous surface, and is given by Eqs. (4) and (5):

$$q_e = K_F C_e^{1/n} \qquad \text{(non-linear form)} \tag{4}$$

$$\log q_e = \log K_F + \frac{1}{n} \log C_e \qquad \text{(linear form)} \tag{5}$$

where K_F is a Freundlich constant representing the relative adsorption capacity of the adsorbent, and n is related to adsorption intensity.

The linear plots of Langmuir and Freundlich isotherm equations are shown in Figs. 6c and d, respectively.

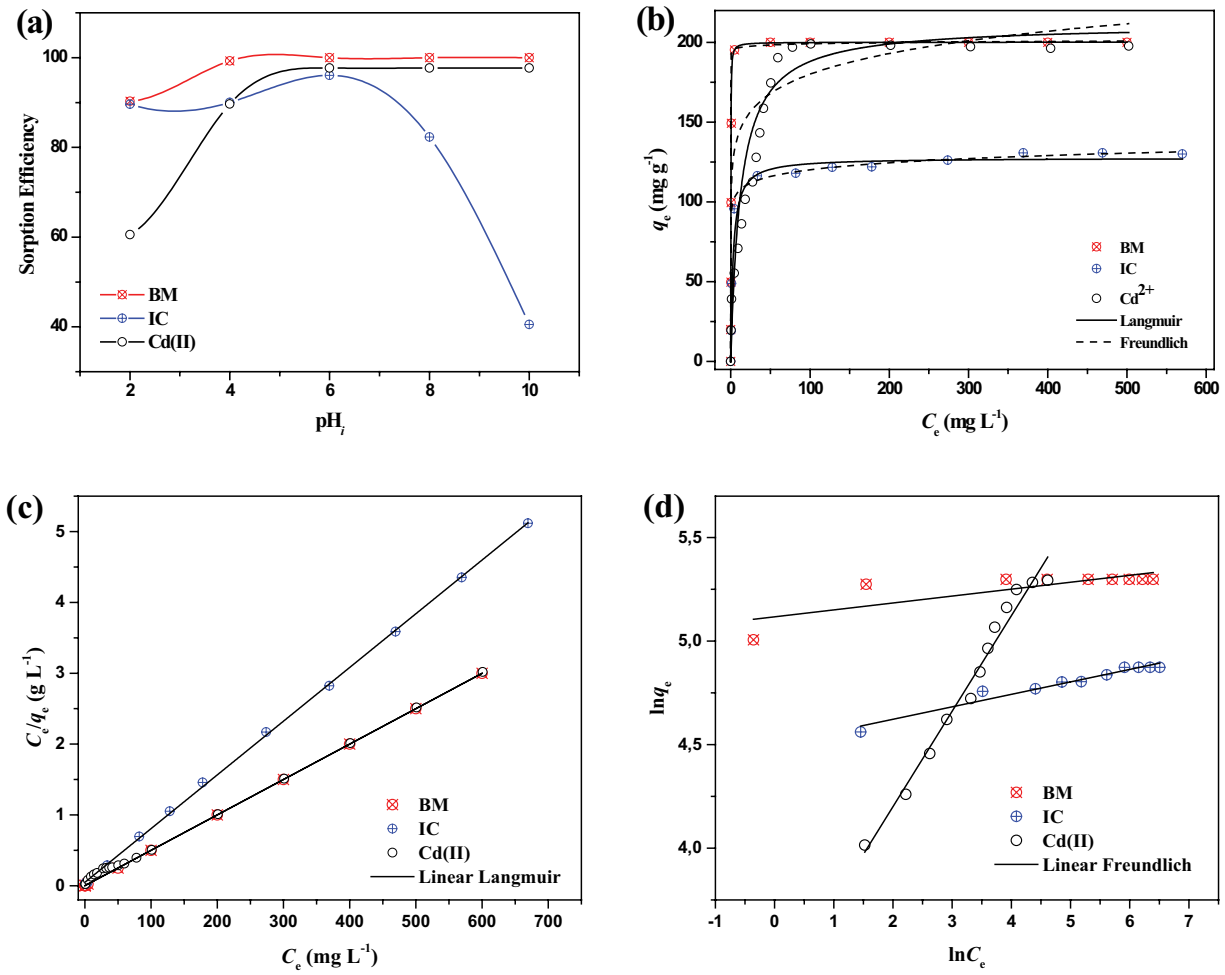

Fig. 6. (a) Effect of pH on sorption of Cd^{2+}, bezaktiv marine and indigo carmine on SATS. Conditions: initial sorbate concentration of 20 mg/L, adsorbent dose of 1 g/L, and contact time of 60 min. (b) Adsorption isotherms of Cd^{2+}, bezaktiv marine and indigo carmine for SATS; conditions: pH 6, initial sorbate concentration of 0–800 mg/L, adsorbent dose of 1 g/L, and contact time of 60 min. Linear Langmuir (c) and Freundlich (d) plots for Cd^{2+}, bezaktiv marine and indigo carmine removal by SATS.

Correlation coefficients (R^2) indicated that the experimental data for Cd(II), BM and IC dyes are better described by the Langmuir adsorption isotherm rather than the Freundlich model (Table 1). In fact, the correlation of data with the linear expression of Langmuir equation gave straight lines over the whole concentration range with excellent correlation coefficients. Based on the Langmuir model, SATS material showed a higher adsorption capacity for all the three pollutants and maximum adsorption capacities found are in the order of 204.08, 142.85, and 200 mg g^{-1} for Cd(II), IC and BM dyes, respectively. These results reflect the homogeneous nature of the surface of the functionalized lignocellulosic adsorbent, making the acetate functional groups on SATS material more available as active sorption sites. Compared with other sorbent materials, SATS showed better sorption capacities for cadmium ions and indigo carmine. Table 2 reports some sorption capacities of different adsorbents for Cd^{2+} and IC dye.

The adsorption capacities of the different adsorbents for cadmium ions and IC dye ranged between 21.6 and 200 mg g^{-1} and 32.8 and 213.2 mg g^{-1}, respectively. The values found in the present work are quite similar to the highest values obtained with succinylated olive stone wastes for Cd^{2+} [38], and with a quaternized hyperbranched polymer for IC dye [42]. Besides, SATS sorbent showed fastest equilibrium time (t_{eq}) among other materials we have compared (Table 2). These results showed that the synthesized SATS sorbent has potential applicability in the removal of heavy metals and dyes from water.

3.3. Adsorption kinetics

For initial Cd(II) and BM, IC dyes concentrations of 20 mg L^{-1} at initial pH 6 as a function of contact time, the adsorption kinetics for SATS is shown in Fig. 7a. Within 2 min of contact time, up to 95.45% of cationic BM dye was adsorbed onto SATS material, whereas 91.15% of Cd^{2+} was sequestered by SATS from the solution, during the same time interval. As shown in Fig. 7a, the results revealed that BM dye removal process reaches equilibrium in 20 min while that of cadmium ions require 30 min. Similarly, the rate of anionic IC dye uptake onto SATS is notably high

Table 1
Adsorption parameters for the sorption of Cd(II), BM and IC dyes onto SATS

Pollutants	Langmuir isotherm constants			Freundlich isotherm constants		
	q_m (mg g^{-1})	b (L mg^{-1})	R^2	K_F (L g^{-1})	$1/n$	R^2
BM	200	4.31	1	166.83	0.033	0.645
IC	142.85	0.148	0.999	90.19	0.060	0.956
Cd(II)	204.08	0.089	0.999	26.52	0.460	0.978

Table 2
Comparison of Cd^{2+} and IC dye sorption capacities using different sorbent materials

Adsorbent	Pollutant	pH	t_{eq} (h)	q_m (mg g^{-1})	Ref
Switchgrass biochar	Cd^{2+}	5	24	34	[35]
Sludge biosorbent	Cd^{2+}	6	1	100	[36]
Water hyacinth biosorbent	Cd^{2+}	6.5	216	21.6	[4]
Marine macroalgae Pelvetia	Cd^{2+}	4.5	24	140	[19]
Succinylated cellulose	Cd^{2+}	6.2	1	178.6	[37]
Succinylated olive stones wastes	Cd^{2+}	4	1	200	[38]
SATS	Cd^{2+}	6	1	204.08	This work
Fe-zeolitic tuff	IC	6.5	40	32.83	[39]
Sewage sludge carbon	IC	6.5	40	92.83	[39]
LDH nanoparticles	IC	9.5.	na	55.5	[40]
Ocimum gratissimum leave	IC	2	2	77.52	[41]
Hyperbranched polymer	IC	6.5	3	213.22	[42]
SATS	IC	6	1	142.85	This work

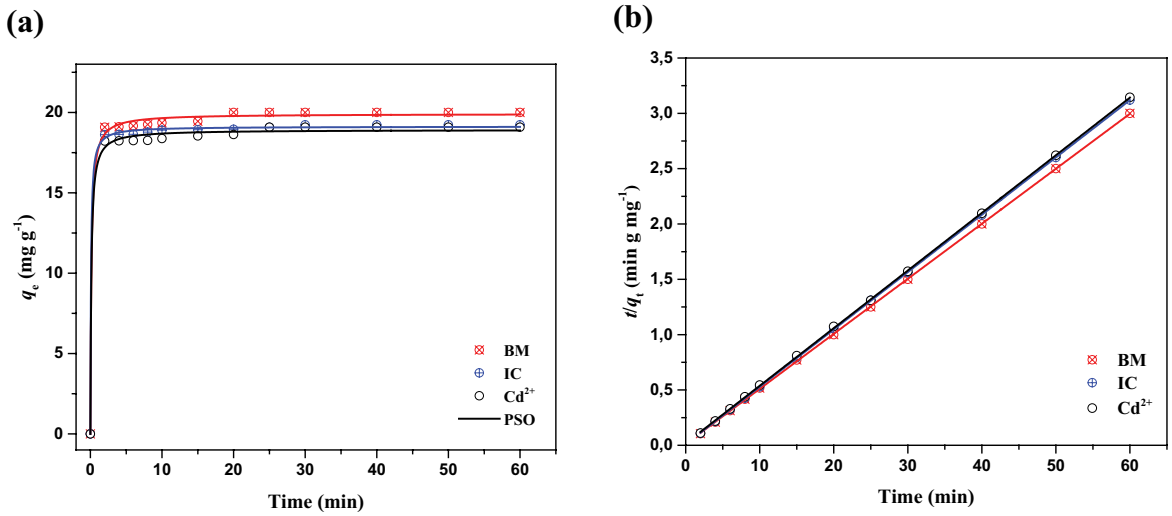

Fig. 7. (a) Adsorption kinetics of Cd^{2+}, bezaktiv marine and indigo carmine onto SATS; Conditions: initial pollutant concentration of 20 mg/L, adsorption dose of 1 g/L, pH 6, contact time of 60 min. (b) Kinetic data fitted to the pseudo-second order kinetic model.

that maximum dye (93.19%) was sorbed from the solution within 2 min of contact time. Overall, 96% of the ultimate adsorption of IC occurs within 30 min of contact time.

The fast adsorption rate of SATS is probably due to the availability of sufficient reactive adsorption sites and also indicates that the removal process is very likely driven by strong ionic interactions between negatively charged acetate groups anchored at the surface of the material and cadmium ions and cationic BM dye in solution. These results suggest that the determinant stage in the adsorption mechanism is a chemical sorption via ion exchange between the adsorbent and adsorbate.

The experimental kinetic data were well fitted to the pseudo-second-order kinetic model. The linear form of pseudo-second-order model is expressed by Eq. (6):

$$\frac{t}{q_t} = \frac{1}{k_2 q_e^2} + \frac{1}{q_e} t \tag{6}$$

where q_e and q_t represent the adsorbed metal ions and dye compounds on SATS adsorbent (mg g^{-1}) at equilibrium and time t, respectively, and k_2 (g mg^{-1} min^{-1}) is the rate constant. The plots of t/q_t vs. t (Fig. 7b) gave straight lines with excellent correlation coefficients (Table 3), which confirm the applicability of the pseudo-second order equation. Moreover, the calculated q_e values from the model are in full agreement with the experimental values ($q_{e,\exp}$).

3.4. Thermodynamic parameters

The removal of BM, IC and Cd^{2+} by SATS sorbent was studied in the temperature range (298–318 K) to determine the thermodynamic parameters, and the results are summarized in Table 4. The pollutants uptake decreased by increasing the temperature, indicating an exothermic process. The thermodynamic parameters $\Delta G°$, $\Delta H°$ and $\Delta S°$ were calculated by using the following equation [43]:

$$\log K = -\frac{\Delta G°}{RT} = \frac{\Delta S°}{R} - \frac{\Delta H°}{RT} \tag{7}$$

where T is the temperature (K), R is the ideal gas constant (8.314 J mol^{-1} K^{-1}) and K is the equilibrium constant (L mg^{-1}). The van't Hoff plot of ln$K$ vs. $1/T$ gave straight lines. The calculated slope and intercept from the plot were used to determine $\Delta H°$ and $\Delta S°$, respectively (Table 4).

The negative value of $\Delta G°$ (–41.7 to –23.8 kJ mol^{-1}) at each temperature implies a favorable and spontaneous adsorption process and confirms the affinity of SATS material for cadmium ions, BM and IC dyes. Furthermore, the negative values of $\Delta H°$ indicate that the adsorption is exothermic and also suggest that the sorption process is a physical adsorption. The obtained values of $\Delta H°$ for Cd(II) and BM are of the order of −62.7 and −32.6 kJ mol^{-1}, respectively. This suggests that the adsorption process is a physical adsorption enhanced by chemical interactions between both Cd(II) and BM and acetate linkers through ion exchange [44]. In addition, the negative values of $\Delta S°$ revealed the decreased randomness at the solid/solution interface solution for the adsorption of Cd(II) and BM dye. The affinity of SATS adsorbent toward IC dye is also confirmed by the positive value of $\Delta S°$ (62.21 J K^{-1} mol^{-1}), which indicates an increase in the degree of freedom of the adsorbed IC molecules and suggests the increased randomness at the solid/solution interface with some structural changes in the adsorbate and the adsorbent. Similar results have been recently reported by Hevira et al. [45] for the biosorption of indigo carmine by *Terminalia catappa* shell, and by Sirajudheen et al. [46] for the removal of indigo carmine by La(III) supported carboxymethylcellulose-clay composite.

Table 3
Kinetic data of Cd(II), BM and IC adsorption onto SATS fitted to the pseudo-second order model

Pollutant	$q_{e,\exp}$	$q_{e,\text{calc}}$	k_2	R^2
	(mg g^{-1})	(mg g^{-1})	(g mg^{-1} min^{-1})	
BM	20.00	20.10	0.192	0.999
IC	19.23	19.29	0.254	0.999
Cd^{2+}	19.08	19.20	0.159	0.999

3.5. Effect of ionic strength on sorption of BM and IC dyes

The influence of ionic strength on adsorption performance of SATS was performed by addition of NaCl to dye solutions since textile wastewaters usually contain inorganic salts to improve the dyeing process. The adsorption selectivity for BM and IC dyes was assessed in the presence of 1–5 mol L^{-1} sodium chloride solutions, as shown in Fig. 8. At 1 M NaCl solution, SATS selectively and totally removed BM (100%) and up to 96% of IC from the solution. As can be seen, the increase of ionic strength in solution (up to 5 mol L^{-1}) has a negligible effect on the adsorption performance of SATS. The removal rate decreased from 100% to 99.62% and from 96% to 84% for BM and IC dyes, respectively. These results demonstrate that the presence of salt has no substantial effect on the adsorption of BM and IC dyes onto SATS, thus lowering its adsorption capacity by only 0.4%–12%.

3.6. Desorption and reusability

Regeneration of the adsorbent makes it economic since reusing the material would reduce the costs associated with its processing and synthesis. To confirm the recyclability and stability of SATS, repeated cycles of adsorption–regeneration tests were carried out. In each cycle, the experimental conditions for the adsorption step were kept the same. After each adsorption step, SATS material was regenerated by washing with aqueous solutions of

Table 4
Thermodynamic parameters for Cd(II), BM and IC sorption onto SATS

Pollutants	$\Delta H°$	$\Delta S°$	$\Delta G°$ (kJ mol^{-1})		
	(kJ mol^{-1})	(J K^{-1} mol^{-1})	298 K	308 K	318 K
BM	–32.658	–21.680	–26.197	–25.980	–25.763
IC	–22.553	62.216	–41.093	–41.715	–42.337
Cd(II)	–62.707	–122.198	–26.291	–25.070	–23.848

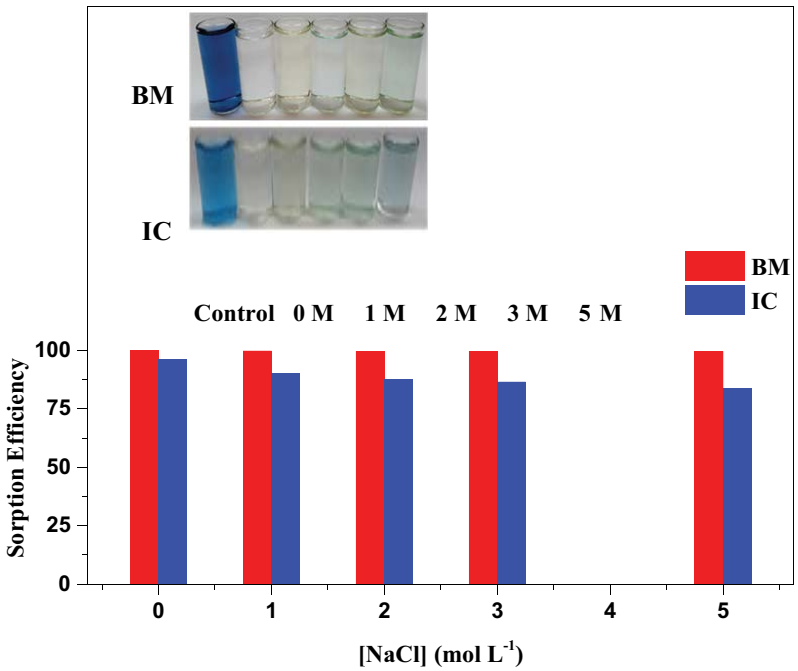

Fig. 8. Effect of ionic strength on the removal efficiency of BM and IC dyes by SATS. Conditions: initial dye concentration of 20 mg/L, adsorption dose of 1 g/L, sodium chloride concentration (1–5 mol L^{-1}), pH 6, contact time of 60 min.

sodium chloride (1 M), sodium hydroxide (1 M) and acidified ethanol for desorption of cadmium ions, BM and IC dyes, respectively. Total desorption was achieved by vigorous stirring during 15 min for both dyes and 60 min for cadmium ions. Fig. 9a shows that at the end of the third repeated cycle, SATS material constantly retains its sorption efficiency and allows obtaining a removal rate of 98%, 94% and 87% for bezaktiv marine, cadmium ions and indigo carmine, respectively. Thus, these results demonstrated that after three repeated cycles there was a slight decrease in the adsorption capacity of SATS, suggesting that the sorbent has excellent regenerability over extended periods of use.

3.7. Adsorption mechanism

Adsorption mechanisms between SATS adsorbent and Cd(II), cationic BM dye and anionic IC dye may include ion exchange, weak coulombic attractions, and electrostatic interactions. The rapid sorption process, reaching equilibrium within 2–20 min of contact time, indicates the involvement of ion exchange process via weak intermolecular forces between the functional acetate groups and ionic species. Therefore, the sequestration of cadmium ions and bezaktiv marine takes place by the release of sodium ions, initially bound to the sodium acetate groups present at the surface of SATS, which indicates that the binding mechanism is an ion exchange process. Moreover, the sorbed amount of Cd^{2+} (1.82 mmol g^{-1}) onto SATS was in good agreement with sodium acetate groups content (3.73 mmol g^{-1}), which indicates an ion exchange process with a stoichiometric ratio 2:1 between monovalent Na^{+} and divalent Cd^{2+}. Similarly, the desorption experiments demonstrated that either sodium chloride or sodium hydroxide aqueous solutions were able to desorb entirely cadmium ions and bezaktiv marine from the exhausted SATS quite rapidly. In order to ascertain the major contribution of functional acetate groups linked to the lignocellulosic matrix of SATS, during the sorption of Cd(II) and the dyes, the termini carboxylate groups were blocked by esterification of SATS with iodomethane. As shown in Fig. 9b, the esterified material MATS exhibited a drastic decrease in its sorption efficiency for all the three pollutants compared with its precursor SATS. Indeed, the methyl ester MATS shows an equilibrium uptake capacity of 23% for Cd^{2+}, 30% for BM and 10% for IC, values which are far lower than those obtained with the un-esterified SATS. These results clearly demonstrate that acetate groups present at the surface of SATS are determinant in the sorption process. The lower sorption capacities obtained for Cd^{2+} and BM with MATS suggest the presence of acidic functional groups even after esterification as confirmed by the pH_{PZC} value (4.42). Therefore, the surface of MATS is negatively charged during the sorption experiments set at pH 6, so the removal of these positively charged species is promoted via weak electrostatic interactions. On the other hand, the exceptionally low removal rate of IC is undoubtedly due to highest electrostatic repulsive interactions between the anionic dye molecules and the negatively charged surface of the MATS adsorbent.

In contrast, the removal of anionic IC dye by SATS is definitely governed by a mechanism other than that of ion exchange since desorption assays have shown that sodium ions (NaOH or NaCl) were not so effective in desorbing IC-loaded SATS. The sorption study was carried out at pH 6, so SATS adsorbent has an overall positive charge (pH_{PZC} = 8.5), and therefore electrostatic attraction is very likely to be the dominant adsorption mechanism between SATS and the anionic IC dye.

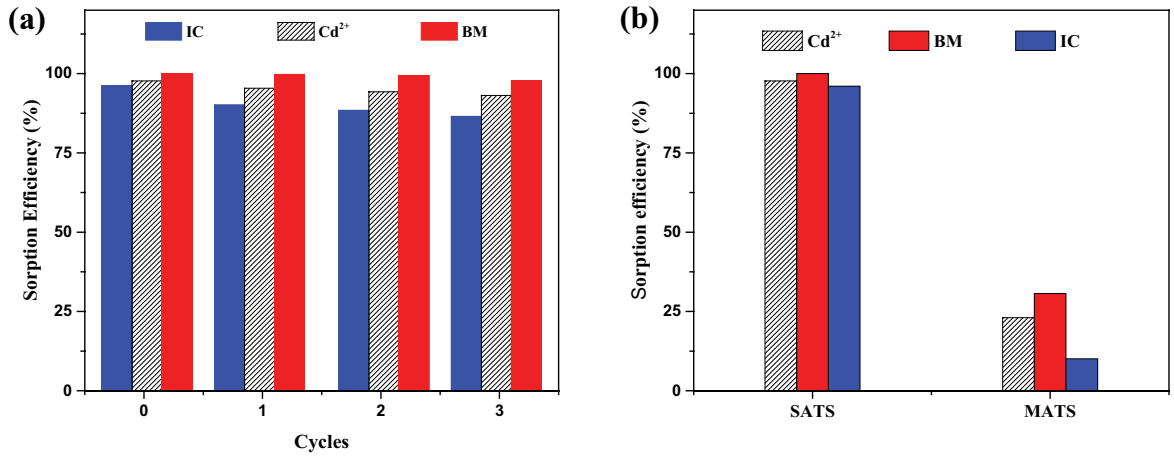

Fig. 9. (a) Removal efficiency of SATS for the sorption of Cd(II), BM and IC dyes over three repeated cycles. (b) Comparison of SATS and MATS materials for the sorption of Cd(II), BM and IC. Conditions: initial pollutant concentration of 20 mg/L, adsorption dose of 1 g/L, pH 6, contact time of 60 min.

4. Conclusions

Novel sodium acetate functionalized lignocellulosic adsorbent SATS derived from a low value by-product of the timber industry was synthesized and evaluated for the removal of cadmium ions and basic/acid dyes in water. Based on the equilibrium adsorption studies, it was found that SATS exhibited higher adsorption capacity for all the three pollutants compared with other sorbent materials as well as faster equilibrium time. The adsorption data fitted well to the Langmuir model and sorption kinetic was found to follow the pseudo-second order model. The calculated thermodynamic parameters indicated the exothermic and spontaneous nature of the removal process. SATS showed high selectivity for the dyes in the presence of inorganic salts in water. The dominant adsorption mechanism is likely to be governed by ion exchange between the sodium acetate linkers anchored at the surface of the adsorbent and cationic species BM and Cd(II), whereas anionic IC removal process may occur via electrostatic interactions between dye molecules and the positively charged surface of SATS material. The adsorbent also showed high performance over repeated use without deterioration in sorption effectiveness. The results from this study show that SATS material could be a promising adsorbent for removing metal ions and cationic/anionic dyes in water and wastewater.

References

[1] Y.A. El-Amier, A.A. Elnaggar, M.A. El-Alfy, Evaluation and mapping spatial distribution of bottom sediment heavy metal contamination in Burullus Lake, Egypt, Egypt. J. Basic Appl. Sci., 4 (2017) 55–66.
[2] T. Akar, B. Anilan, A. Gorgulu, S.T. Akar, Assessment of cationic dye biosorption characteristics of untreated and non-conventional biomass: pyracantha coccinea berries, J. Hazard. Mater., 168 (2009) 1302–1309.
[3] J.O. Esalah, M.E. Weber, J.H. Vera, Removal of lead, cadmium and zinc from aqueous solutions by precipitation with sodium Di(n-Octyl) phosphinate, Can. J. Chem. Eng., 78 (2000) 948–954.
[4] M. Li, X. Xiao, S. Wang, X. Zhang, J. Li, S.G. Pavlostathis, X. Luo, S. Luo, G. Zeng, Synergistic removal of cadmium and organic matter by a microalgae endophyte symbiotic system (MESS): an approach to improve the application potential of plant-derived biosorbents, Environ. Pollut., 261 (2020) 114177.
[5] T.D.A. Maranhão, D.L.G. Borges, M.A.M.S. da Veiga, A.J. Curtius, Cloud point extraction for the determination of cadmium and lead in biological samples by graphite furnace atomic absorption spectrometry, Spectrochim. Acta B, 60 (2005) 667–672.
[6] S. Boubakri, M.A. Djebbi, Z. Bouaziz, P. Namour, N. Jaffrezic-Renault, A.B.H. Amara, M. Trabelsi-Ayadi, I. Ghorbel-Abid, R. Kalfat, Removal of two anionic reactive textile dyes by adsorption into MgAl-layered double hydroxide in aqueous solutions, Environ. Sci. Pollut. Res., 25 (2018) 23817–23832.
[7] S. Pourfadakari, N. Yousefi, A.H. Mahvi, Removal of Reactive Red 198 from aqueous solution by combined method multi-walled carbon nanotubes and zero–valent iron: equilibrium, kinetics, and thermodynamic, Chin. J. Chem. Eng., 24 (2016) 1448–1455.
[8] G.D. Degermenci, N. Degermenci, V. Ayvaoglu, E. Durmaz, D. Çakır, E. Akan, Adsorption of reactive dyes on lignocellulosic waste; characterization, equilibrium, kinetic and thermodynamic studies, J. Clean. Prod., 225 (2019) 1220–1229.
[9] T.A. Kurniawan, G.Y. Chan, W.H. Lo, S. Babel, Physico-chemical treatment techniques for wastewater laden with heavy metals, Chem. Eng. J., 118 (2006) 83–98.
[10] S.M. Doke, G.D. Yadav, Novelties of combustion synthesized titania ultrafiltration membrane in efficient removal of methylene blue dye from aqueous effluent, Chemosphere, 117 (2014) 760–765.
[11] J.B. Tarkwa, N. Oturan, E. Acayanka, S. Laminsi, M.A. Oturan, Photo-fenton oxidation of Orange G azo dye: process optimization and mineralization mechanism, Environ. Chem. Lett., 17 (2019) 473–479.
[12] M.S. Secula, A. Vajda, B. Cagnon, F. Warmont, I. Mamaliga, Photo-Fenton-peroxide process using FE (II)-embedded composites based on activated carbon: characterization of catalytic tests, Can. J. Chem. Eng., 98 (2019) 650–658.
[13] A.A. El-Bindary, S.M. El-Marsafy, A.A. El-Maddah, Enhancement of the photocatalytic activity of ZnO nanoparticles by silver doping for the degradation of AY99 contaminants, J. Mol. Struct., 1191 (2019) 76–84.
[14] G. Sharma, A. Kumar, S. Sharma, Mu. Naushad, P. Dhiman, D.V.N. Vo, F.J. Stadler, Fe_3O_4/ZnO/Si_3N_4 nanocomposite based photocatalyst for the degradation of dyes from aqueous solution, Mater. Lett., 278 (2020) 128359.
[15] C. Moreno-Castilla, M.A. Álvarez-Merino, M.V. López-Ramón, J. Rivera-Utrilla, Cadmium ion adsorption on different carbon

adsorbents from aqueous solutions. Effect of surface chemistry, pore texture, ionic strength, and dissolved natural organic matter, Langmuir, 20 (2004) 8142–8148.
[16] M.A. Fontecha-Cámara, M.V. López-Ramón, M.A. Álvarez-Merino, C. Moreno-Castilla, Effect of surface chemistry, solution ph, and ionic strength on the removal of herbicides diuron and amitrole from water by an activated carbon fiber, Langmuir, 23 (2007) 1242–1247.
[17] A. Kaya, Adsorption studies of Cibacron Blue onto both untreated and chemically treated pistachio shell powder from aqueous solutions, Sep. Sci. Technol., 55 (2020) 1–16.
[18] M.A. Ahmad, N.S. Afandi, K.A. Adegoke, O.S. Bello, Optimization and batch studies on adsorption of malachite green dye using rambutan seed activated carbon, Desal. Wat. Treat., 57 (2015) 1–25.
[19] F.V. Hackbarth, F. Girardi, S.M.A. GuelliU. de Souza, A.A.U. de Souza, R.A.R. Boaventura, V.J.P. Vilar, Marine macroalgae *Pelvetia canaliculata* (Phaeophyceae) as a natural cation exchanger for cadmium and lead ions separation in aqueous solutions, Chem. Eng. J., 242 (2014) 294–305.
[20] P. Thilagavathy, T. Santhi, Kinetics, isotherms and equilibrium study of Co(II) adsorption from single and binary aqueous solutions by *Acacia nilotica* leaf carbon, Chin. J. Chem. Eng., 22 (2014) 1193–1198.
[21] S. Jain, R.V. Jayaram, Removal of basic dyes from aqueous solution by low-cost adsorbent: Wood apple shell (*Feronia acidissima*), Desalination, 250 (2010) 921–927.
[22] U.R. Lakshmi, V.C. Srivastava, I.D. Mall, D.H. Lataye, Rice husk ash as an effective adsorbent: evaluation of adsorptive characteristics for Indigo Carmine dye, J. Environ. Manage., 90 (2009) 710–720.
[23] M. Arami, N.Y. Limaee, N.M. Mahmoodi, Evaluation of the adsorption kinetics and equilibrium for the potential removal of acid dyes using a biosorbent, Chem. Eng. J., 139 (2008) 2–10.
[24] F. Ferrero, Dye removal by low cost adsorbents: Hazelnut shells in comparison with wood sawdust, J. Hazard. Mater., 142 (2007) 144–152.
[25] G. Blazquez, F. Hernainz, M. Calero, L.F. Ruiz-Nunez, Removal of cadmium ions with olive stones: the effect of somes parameters, Process Biochem., 40 (2005) 2649–2654.
[26] L.V.F. Oliveira, S. Bennici, L. Josien, L. Limousy, M.A. Bizeto, F.F. Camilo, Free-standing cellulose film containing manganese dioxide nanoparticles and its use in discoloration of Indigo Carmine dye, Carbohydr. Polym., 230 (2020) 115621.
[27] L-X. Zhong, X.W. Peng, D. Yang, R.C. Sun, Adsorption of heavy metals by a porous bioadsorbent from lignocellulosic biomass reconstructed in an ionic liquid, J. Agric. Food Chem., 60 (2012) 5621–5628.
[28] Y. Djilali, E.H. Elandaloussi, A. Aziz, L-C. de Ménorval, Alkaline treatment of timber sawdust: a straightforward route toward effective low-cost adsorbent for the enhanced removal of basic dyes from aqueous solutions, J. Saudi Chem. Soc., 20 (2016) S241–S249.
[29] A.K. Meena, K. Kadirvelu, G.K. Mishra, C. Rajagopal, P.N. Nagar, Adsorptive removal of heavy metals from aqueous solution by treated sawdust (*Acacia arabica*), J. Hazard. Mater., 150 (2008) 604–611.
[30] M.A.K.M. Hanafiah, W.S.W. Ngah, S.H. Zolkafly, L.C. Teong, Z.A. Abdul Majid, Acid Blue 25 adsorption on base treated *Shorea dasyphylla* sawdust: kinetic, isotherm, thermodynamic and spectroscopic analysis, J. Environ. Sci., 24 (2012) 261–268.
[31] E.N. Bakatula, D. Richard, C.M. Neculita, G.J. Zagury, Determination of point of zero charge of natural organic materials, Environ. Sci. Pollut. Res., 25 (2018) 7823–7833.
[32] M.N.M. Ibrahim, M.R.A. Haras, C.S. Sipaut, H.Y. Aboul-Enein, A.A. Mohamed, Preparation and characterization of a newly water soluble lignin graft copolymer from oil palm lignocellulosic waste, Carbohydr. Polym., 80 (2010) 1102–1110.
[33] Z. Yang, Z.H. Jiang, C.L. So, C.Y. Hse, Rapid prediction of wood crystallinity in Pinus elliotii plantation wood by near-infrared spectroscopy, J. Wood Sci., 53 (2007) 449–453.
[34] M.G. Gronli, G. Varhegyi, C. Di Blasi, Thermogravimetric analysis and devolatilization kinetics of wood, Ind. Eng. Chem. Res., 41 (2002) 4201–4208.
[35] P. Regmi, J.L.G. Moscoso, S. Kumar, X. Cao, J. Mao, G. Schafran, Removal of copper and cadmium from aqueous solution using switchgrass biochar produced via hydrothermal carbonization process, J. Environ. Manage., 109 (2012) 61–69.
[36] N.E.H. Larbi, D.R. Merouani, H. Aguedal, A. IDDOU, A. Khelifa, Removal of heavy mMetals Cd(II) and Al(III) from aqueous solutions by an eco-friendly biosorbent, Key Eng. Mater., 800 (2019) 181–186.
[37] B. Belhalfaoui, A. Aziz, E.H. Elandaloussi, M.S. Ouali, L.C. De Ménorval, Succinate-bonded cellulose: a regenerable and powerful sorbent for cadmium-removal from spiked high-hardness groundwater, J. Hazard. Mater., 169 (2009) 831–837.
[38] A. Aziz, E.H. Elandaloussi, B. Belhalfaoui, M.S. Ouali, L.C. De Ménorval, Efficiency of succinylated-olive stone biosorbent on the removal of cadmium ions from aqueous solutions, Colloids Surf. B, 73 (2009) 192–198.
[39] E. Gutiérrez-Segura, M. Solache-Ríos, A. Colin-Cruz, Sorption of indigo carmine by a Fe-zeolitic tuff and carbonaceous material from pyrolyzed sewage sludge, J. Hazard. Mater., 170 (2009) 1227–1235.
[40] M.A. Ahmed, A.A. brick, A.A. Mohamed, An efficient adsorption of indigo carmine dye from aqueous solution on mesoporous Mg/Fe layered double hydroxide nanoparticles prepared by controlled sol-gel route, Chemosphere, 174 (2017) 280–288.
[41] A.O. Dada F.A. Adekola, E.O. Odebunmi, F.E. Dada, O.M. Bello, B.A. Akinyemi, O.S. Bello, O.G. Umukoro, Sustainable and low-cost *Ocimum gratissimum* for biosorption of indigo carmine dye: kinetics, isotherm, and thermodynamic studies, Int. J. Phytorem., 22 (2020) 1524–1537.
[42] M. Bendjelloul, E.H. Elandaloussi, L.-C. de Ménorval, A. Bentouami, Quaternized triethanolamine-sebacoyl moieties in highly branched polymer architecture as a host for the entrapment of acid dyes in aqueous solutions, J. Water Reuse Desal., 7 (2017) 53–65.
[43] D. Liua, Z. Huanga, M. Li, X. Li, P. Sun, L. Zhou, Construction of magnetic bifunctional β-cyclodextrin nanocomposites for adsorption and degradation of persistent organic pollutants, Carbohydr. Polym., 230 (2020) 115564.
[44] F. Renault, N. Morin-Crini, F. Gimbert, P.M. Badot, G. Crini, Cationized starch-based material as a new ion-exchanger adsorbent for the removal of C.I. Acid Blue 25 from aqueous solutions, Bioresour. Technol., 99 (2008) 7573–7586.
[45] L. Hevira, Zilfa, Rahmayenid, J.O. Ighalo, R. Zein, Biosorption of indigo carmine from aqueous solution by *Terminalia Catappa* shell, J. Environ. Chem. Eng., 8 (2020) 104290.
[46] P. Sirajudheen, P. Karthikeyan, S. Vigneshwaran, S. Meenakshi, Synthesis and characterization of La(III) supported carboxymethylcellulose-clay composite for toxic dyes removal: Evaluation of adsorption kinetics, isotherms and thermodynamics, Int. J. Biol. Macromol., 161 (2020) 1117–1126.